BJA

British Journal of Anaesthesia, 125 (1): 67–76 (2020)

doi: 10.1016/j.bja.2020.03.014
Advance Access Publication Date: 24 April 2020
Neuroscience and Neuroanaesthesia

Dynamic changes in rhythmic and arrhythmic neural signatures in the subthalamic nucleus induced by anaesthesia and tracheal intubation

Yongzhi Huang[1,*,†], Kejia Hu[2,†], Alexander L. Green[1], Xin Ma[3], Martin J. Gillies[1], Shouyan Wang[4], James J. Fitzgerald[1], Yixin Pan[2], Sean Martin[1], Peng Huang[2], Shikun Zhan[2], Dianyou Li[2], Huiling Tan[5,6,**], Tipu Z. Aziz[1] and Bomin Sun[2,***]

[1]Nuffield Department of Surgical Sciences, John Radcliffe Hospital, University of Oxford, Oxford, UK, [2]Center of Functional Neurosurgery, Ruijin Hospital, Shanghai Jiao Tong University School of Medicine, Shanghai, China, [3]Department of Anesthesiology, Ruijin Hospital, Shanghai Jiao Tong University School of Medicine, Shanghai, China, [4]Institute of Science and Technology for Brain-Inspired Intelligence, Fudan University, Shanghai, China, [5]Medical Research Council Brain Network Dynamics Unit at the University of Oxford, Oxford, UK and [6]Nuffield Department of Clinical Neurosciences, John Radcliffe Hospital, University of Oxford, Oxford, UK

*Corresponding authors. E-mails: yongzhi.huang@nds.ox.ac.uk, huiling.tan@ndcn.ox.ac.uk, sbm11224@rjh.com.cn

†These authors contributed equally to this work.

Abstract

Background: Subcortical structures, including the basal ganglia, have been proposed to be crucial for arousal, consciousness, and behavioural responsiveness. How the basal ganglia contribute to the loss and recovery of consciousness during anaesthesia has, however, not yet been well characterised.

Methods: Twelve patients with advanced Parkinson's disease, who were undergoing deep brain stimulation (DBS) electrode implantation in the subthalamic nucleus (STN), were included in this study. Local field potentials (LFPs) were recorded from the DBS electrodes and EEG was recorded from the scalp during induction of general anaesthesia (with propofol and sufentanil) and during tracheal intubation. Neural signatures of loss of consciousness and of the expected arousal during intubation were sought in the STN and EEG recordings.

Results: Propofol–sufentanil anaesthesia resulted in power increases in delta, theta, and alpha frequencies, and broadband power decreases in higher frequencies in both STN and frontal cortical areas. This was accompanied by increased STN–frontal cortical coherence only in the alpha frequency band (119 [68]%; $P=0.0049$). We observed temporal activity changes in STN after tracheal intubation, including power increases in high-beta (22–40 Hz) frequency (98 [123]%; $P=0.0064$) and changes in the power-law exponent in the power spectra at lower frequencies (2–80 Hz), which were not observed in the frontal cortex. During anaesthesia, the dynamic changes in the high-gamma power in STN LFPs correlated with the power-law exponent in the power spectra at lower frequencies (2–80 Hz).

Conclusions: Apart from similar activity changes in both STN and cortex associated with anaesthesia-induced unresponsiveness, we observed specific neuronal activity changes in the STN in response to the anaesthesia and tracheal intubation. We also show that the power-law exponent in the power spectra in the STN was modulated by tracheal intubation in anaesthesia. Our results support the hypothesis that subcortical nuclei may play an important role in the loss and return of responsiveness.

Keywords: anaesthesia; consciousness; electrophysiology; local field potential; power law; propofol; subthalamic nucleus; tracheal intubation

Received: 6 September 2019; **Accepted:** 19 March 2020

Editor's key points

- The mechanisms by which the basal ganglia contribute to consciousness, arousal, and behavioural responses are not clear.
- Deep brain stimulation of the subthalamic nuclei, which form part of the basal ganglia system, is a common treatment for Parkinson's disease.
- The authors recorded local field potentials from the subthalamic nucleus (STN) and the EEG from the scalp during induction of anaesthesia and tracheal intubation.
- Changes were observed in the power spectrum, coherence and power-law distribution in the spectra during loss of consciousness and during the expected arousal of intubation in the STN and EEG.

Understanding of the alteration of brain states under general anaesthesia has been significantly advanced by recent electrophysiology and functional neuroimaging studies. Anaesthetic-induced unconsciousness is thought to be associated with changes in different neural oscillations in cortical brain areas, commonly monitored by scalp EEG. For example, increase in global slow-wave oscillation (SWO) power,[1,2] increase in frontal alpha power,[1,3,4] burst suppression,[5,6] and changes in coherence[1,3] were observed during induction of unconsciousness with propofol, one of the most commonly used anaesthetic drugs. Numerous neuroimaging studies have also shown that several subcortical brain structures are involved in altered arousal and unconsciousness,[7–9] and it is suggested that the disruption of communication between the cortical and subcortical structures plays a crucial role in anaesthetic-induced unconsciousness.[8,10,11] A recent study by Nir and colleagues[12] revealed that there was a transient increase in functional connectivity between brainstem arousal nuclei around the point of regaining responsiveness to verbal command, suggesting that the emergence from propofol-induced sedation is an active subcortically driven process. Sleigh and Warnaby[13] further hypothesised that these subcortical nuclei are the starter motors, even though may not be the main engine of consciousness. It was speculated that the combination of increase in activity in both cortical and subcortical areas and a sudden, short-lived surge in coherence amongst brainstem nuclei is the characteristic signature of a network undergoing a connectivity phase transition in its dynamics. Therefore, investigating subcortical changes and neuronal network-level effects induced by anaesthetic drugs has become compelling and necessary for better understanding the neuronal mechanism of how general anaesthetics cause loss of consciousness.[14–16]

The basal ganglia are important subcortical structures composed of the striatum, globus pallidus, subthalamic nucleus (STN), and substantia nigra, and have connection with a wide range of cortical areas, including the frontal cortex[17,18] and the brainstem.[19,20] A growing amount of studies start to highlight the importance of cortico-basal ganglia-thalamo-cortical network in arousal and consciousness.[21–24] A recent investigation on the connectivity within the cortico-basal ganglia-thalamo-cortical network has shown that propofol-induced unconsciousness modulated the pallidal connectivity to the posterior cingulate cortex, suggesting the role of pallido-cortical connectivity in altered states of consciousness.[23] A recent study also showed that propofol significantly modulated the oscillatory neuronal activity in the beta-frequency band in the STN.[25] However, all those changes in STN reported earlier are similar to those observed from the frontal cortex. In this study, we sought for signatures in the STN, but not observable in the frontal cortex, that reflected the altered responsiveness and arousal during anaesthetic-induced anaesthesia and tracheal intubation.

Electrophysiological brain activity consists of rhythmic oscillation and arrhythmic activity indicative of the oscillatory and fractal dynamics, respectively, arising from likely distinct neural basis.[26–28] Up to now, most of the electrophysiological research on anaesthesia has focused on narrowband oscillatory activity patterns. Meanwhile, arrhythmic brain activity coexists with brain oscillations and accounts for the majority of the signal power recorded in LFP/EEG/magnetoencephalography (MEG), but our understanding of it remains very limited. The arrhythmic activity often appears with two spectral profiles: broadband and scale free.[29] The power spectrum of scale-free dynamics tends to follow a power-law distribution: $P \sim 1/f^{\beta}$,[26,28,30,31] which means the power P tends to fall off with increasing frequency f with β the power-law exponent. Increasing evidence has emerged suggesting that the scale-free features can uncover the functional involvement of neuronal activity in specific states. The power-law exponent has been shown to be modulated by sleep[32] and neurological and psychiatric disorders.[33,34] The changes of power-law exponent during propofol-induced anaesthesia were also observed from human EEG and macaque electrocorticography (ECoG).[35,36]

Here, we recorded electrophysiological signals from STN and frontal cortex simultaneously in patients with Parkinson's disease (PD) undergoing deep brain stimulation (DBS) surgery. We compared the neuronal signatures, including oscillatory activity, power-law distribution, and functional connectivity, in these brain areas under awake, propofol/sufentanil-induced unresponsiveness, and under tracheal intubation in anaesthesia. We hypothesised that both oscillatory and scale-free arrhythmic activities in the STN, and the functional connectivity with cortex will be modulated by altered consciousness in general anaesthesia. In particular, we hypothesised that specific neuronal signatures may emerge in the STN local field potential (LFP), but not observable from the frontal cortex, reflecting the altered arousal in propofol/sufentanil-induced anaesthesia and tracheal intubation.

Methods

Subjects

Twelve patients with advanced PD (24 hemispheres; three females) undergoing bilateral DBS surgery of the STN were included in this study. All subjects gave their written informed consent, and the local ethics committees from Oxford and Shanghai approved the study separately (Oxfordshire REC B: 09/H0605/62; Shanghai Ruijin Hospital Research Ethics Committee: [2019] Clinical Ethical Review No. [236]). Details of the patients are reported in Supplementary Table S1. All recordings in this study were performed when the patients underwent the second-stage operation to implant with a subcutaneous pulse generator under general anaesthesia.

Anaesthetic procedures and data acquisition

The technique for induction of anaesthesia was at the discretion of the attending anaesthetist. In the anaesthetic

room, no pre-anaesthetic medication was administered; an i.v. line of Ringer's lactate solution 10 ml kg^{-1} was infused via 20G venous cannula through the dorsum of the non-dominant hand of the patients. After establishment of standard monitoring (ECG, noninvasive blood pressure, and pulse oximeter), general anaesthesia was induced, in which all patients received sufentanil (0.5 μg kg^{-1}) 60 s before propofol. Loss of responsiveness (LOR) was achieved by i.v. propofol (1–2 mg kg^{-1}). Time to LOR was determined by checking every 5 s for the loss of verbal response and eyelash reflex. After LOR, i.v. bolus of rocuronium (0.6 mg kg^{-1}) was given to the patients. Tracheal intubation was performed when no response was yielded with train-of-four stimulation. After tracheal intubation, the lungs were mechanically ventilated and the ventilator settings adjusted to maintain the end-tidal CO_2 partial pressure between 4.7 and 5.3 kPa.

Electrophysiological signals from bilateral STN and frontal cortex were obtained from 3 min before the start of anaesthetic procedure to 2 min after tracheal intubation (11.6 [2.7] min in total for each patient). Signal acquisition was carried out using TMSi Refa system (TMS International, Oldenzaal, Netherlands) with a sampling rate of 2048 Hz (Oxford), or a home-built device with a sampling rate of 1000 Hz (Shanghai). Local field potential signals were recorded with the four contacts of the DBS electrode (0, 1, 2, and 3, with 0 being the deepest contact) using monopolar configuration (Oxford) or bipolar configuration (0–1, 1–2, and 2–3) (Shanghai), with a reference electrode placed on the surface of the mastoid. Bipolar frontal EEG (FP_1–Fz or FP_2–Fz) was recorded according to the international 10–20 EEG system.

Data pre-processing

Bipolar LFPs (Oxford) were subsequently derived offline by subtracting the monopolar recordings between neighbouring contacts on each electrode. The LFP and EEG data were resampled at 1000 Hz, high-pass filtered at 0.2 Hz, and notch filtered at 50 Hz and the harmonics. The recordings were visually inspected, and those data with noise and artefacts, including excessive movement, muscle artefacts, and jump artefacts, were excluded from further analysis. This led to four out of the 24 STN LFPs during tracheal intubation, and four out of the 12 frontal EEG to be removed from final analysis. The selection of bipolar channel (see details in Supplementary Table S1) for further LFP analysis was based on the review of pre- and postoperative imaging and postoperative clinical programming by the surgical team. Forty seconds of continuous data from each of the following three states was considered for each subject: (i) awake state, before anaesthetic induction; (ii) LOR state, after loss of eyelash reflex and before tracheal intubation; and (iii) intubation state, beginning at 10 s after starting tracheal intubation.

Spectral analysis

Power spectra of the electrophysiological signals (bipolar LFPs and EEGs) were calculated for all subjects in each state (awake, LOR, and intubation) with the multi-taper method using the Chronux toolbox.[37] Multi-taper parameters were set using time window lengths of T=2 s, time-bandwidth product TW=2, and number of tapers K=3, resulting in a spectral resolution of 2 Hz when quantifying the average power spectra of the signal from different consciousness states. Time–frequency decomposition was also estimated to quantify the temporal dynamics of the power spectra by using the multi-taper spectrogram method, with window lengths of 2 s and overlap of 1.5 s, TW=2, and K=3.

Coherence analysis

To describe the connectivity between STN and frontal cortex, the magnitude-squared coherence between STN LFPs and frontal EEG was estimated using the multi-taper method, with window lengths of 4 s, TW=4, and K=7. The magnitude-squared coherence estimate is the normalised cross-spectral density by the power spectral density (PSD) with values between 0 and 1 that indicates the degree of co-variability between the two signals over different frequency ranges. Imaginary coherence, which is only sensitive to synchronisation of two signals that are time lagged to each other, was further estimated to remove volume conduction of common signals. We derived the imaginary coherence between STN LFPs and frontal EEG using similar parameters used for coherence analysis.

Power-law scaling analysis

Arrhythmic activities in the brain LFPs tend to exhibit a 1/f-like spectrum: $P \sim 1/f^{\beta}$. To characterise the property of these neural signals, the power spectrum of neural signals is often fitted by a linear function in a log–log coordinate space, where the slope (β) provides an estimate of the underlying power-law (or frequency-scaling) exponent. Here, we investigated how the power-law exponents in STN LFP and frontal cortical EEG are modulated by alteration of conscious states under general anaesthesia. In addition, rhythmic brain oscillations appear as local peaks that rise above the power-law distribution in the power spectrum, which can confound the real scale-free dynamics, highlighting the importance of making a careful dissociation between rhythmic oscillation and arrhythmic activity.[26,31,38] To estimate an accurate power-law exponent independent from any narrowband oscillations, we first adopted the irregular-resampling auto-spectral analysis (IRASA) method to separate the fractal from oscillatory components of the power spectrum.[38] This method takes advantage of the self-affinity property of a fractal (i.e. scale-free) time series (i.e. the statistical distribution of the data remains unchanged when resampled at different scales). Moreover, to further mitigate the potential effect of remaining spectral peak unsuccessfully removed by the IRASA method, the fractal power spectrum across a frequency range, excluding a narrower frequency band with local spectral peaks, was fitted. Then, the power-law exponent is estimated from the slope of the linear fit.

Here, a sliding time window with a length of 2 s and overlap of 1 s was applied for STN LFP and frontal EEG. Within each time window, the fractal power spectrum and the corresponding power-law exponent were estimated. We further averaged the time courses of the power-law exponents within distinct behavioural states and compared the results across states.

Statistical analysis

For STN LFPs, we determined whether or not there were significant differences of power in oscillatory activities in each frequency band and arrhythmic power-law exponent between awake and LOR states, and between LOR and intubation states.

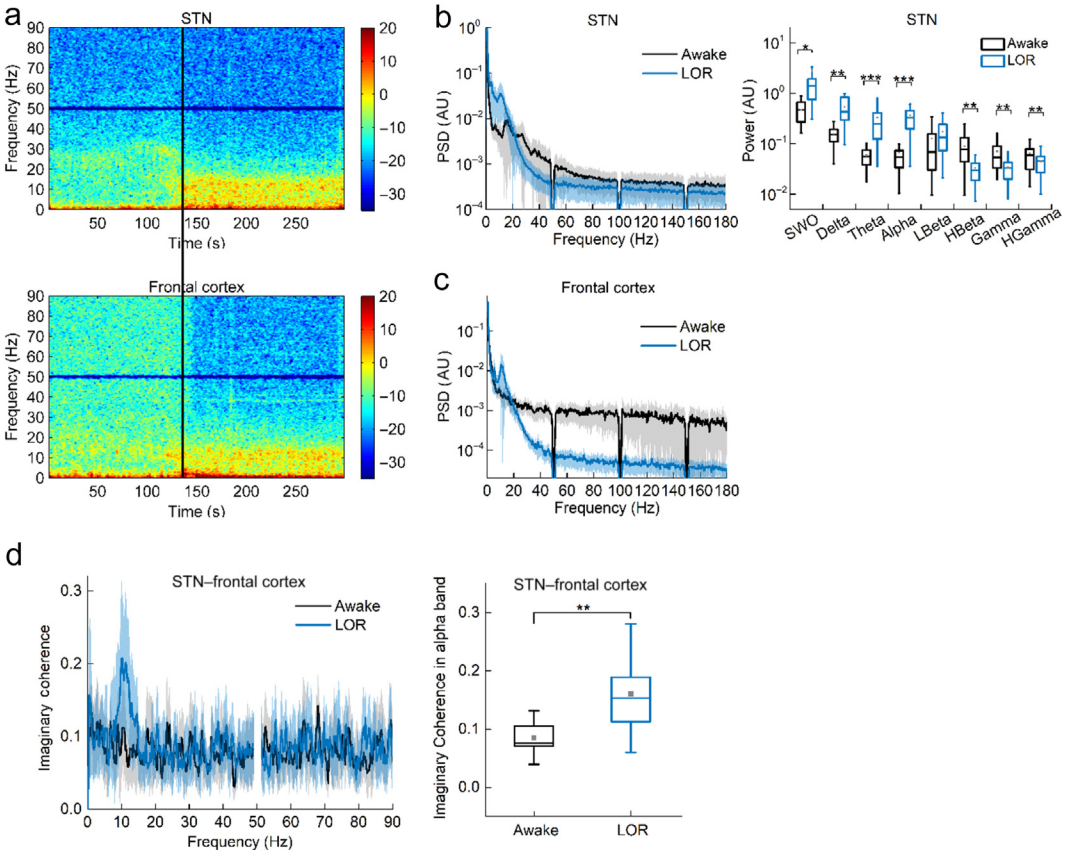

Figure 1. Increased low-frequency activity and reduced high-frequency activities in subthalamic nucleus (STN) during loss of responsiveness (LOR) compared with awake, with the alpha band activity coherent with the frontal cortex. (a) Representative time–frequency spectrograms of STN local field potentials (LFPs) and frontal cortical EEG during the induction of unconsciousness. The vertical black line marks the time of loss of eyelash reflex indicating LOR. (b) Group spectra and box plot showing power in different frequency bands of STN LFPs across all subjects in awake and LOR states. (c) Group spectra of frontal EEG across subjects in awake and LOR states. (d) Group imaginary coherence between STN and frontal cortex across subjects in awake and LOR states. *P<0.05; **P<0.01; ***P<0.001. HBeta, high beta; HGamma, high gamma; LBeta, low beta; PSD, power spectral density; SWO, slow-wave oscillation.

Before comparison, raw values of power and power-law exponent across subjects in each state were examined for deviations from normality using the Kolmogorov–Smirnov test. The power and exponent values were compared between states using the Wilcoxon signed-rank test if the data are not normally distributed, or paired *t*-test if they are normally distributed. For frontal EEG, the statistical significance of the differences of power and power-law exponent between LOR and intubation states was assessed. The imaginary coherence between STN LFPs and frontal EEG in LOR and intubation states was also compared. The resulting *P*-values were accordingly corrected for multiple comparisons with the false discovery rate (FDR) procedure across bands and states. All the signal processing and statistical analysis were conducted using MATLAB (version 9.1; MathWorks, Inc., Natick, MA, USA).

Results

Firstly, the difference in the patient characteristics from two centres was assessed. There was no significant difference between the age of the patients in Oxford (mean [standard deviation {SD}]: 52.3 [10.6] yr) and that in Shanghai (mean [SD]: 56.5 [12.1] yr) (P=0.6; Wilcoxon rank-sum test). Although the weight of the patients between two centres (mean [SD]: 85.2 [13.1] kg in Oxford; 69.6 [6.3] kg in Shanghai) was significantly different (P=0.03; Wilcoxon rank-sum test), the anaesthetic drug was administered based on the patient's weight. Therefore, the subjects recruited from two sites were grouped together for the analysis in this study.

Increased low-frequency oscillatory activity and reduced high-frequency activity in the STN during anaesthesia

We first compared the spectrograms from STN LFP and frontal EEG signals during the transition from awake to unconsciousness. The spectrograms showed dynamic spectral changes during induction of unconsciousness with the most dominant characteristics being the increased power in the alpha oscillation (8–14 Hz) and SWO (0.2–1.5 Hz) in both STN and frontal cortex at LOR state (Fig. 1a). In addition, there was

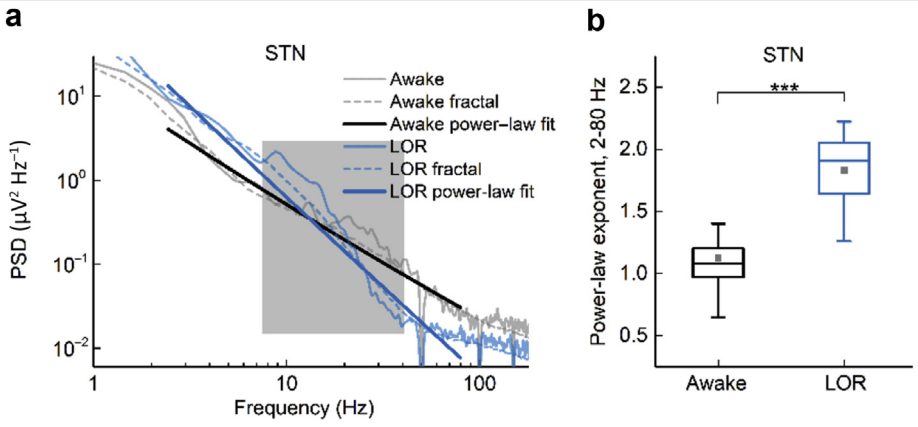

Figure 2. Increased power-law exponent at 2–80 Hz in subthalamic nucleus (STN) local field potentials (LFPs) at loss of responsiveness (LOR) state compared with awake state. (a) Representative power spectra, corresponding fractal components, and power-law fit of the STN LFPs in awake and LOR states. The range with local power peaks was marked by the shadow. (b) Box plot showing power-law exponent in STN LFPs across subjects in awake and LOR states. ***P<0.001. PSD, power spectral density.

also a significant decrease in power in the high-beta (22–40 Hz) and gamma (40–80 Hz) frequency bands in the STN at LOR state (Fig. 1a). Group-level spectra (n=24; 12 subjects) revealed that, compared with the awake state, the power in low frequencies, including SWO, delta (1.5–4 Hz), theta (4–8 Hz), and alpha oscillations, significantly increased; meanwhile, the power in higher frequencies, including high-beta, gamma, and high-gamma (80–180 Hz) bands significantly decreased in the STN at LOR state (SWO: 497 [573]%, P=0.0288; delta: 293 [276]%, P=0.0017; theta: 482 [352]%, P=0.0006; alpha: 533 [352]%, P=0.0005; high beta: 52 [25]%, P=0.0021; gamma: 47 [16]%, P=0.0032; and high gamma: 30 [12]%, P=0.0017; FDR correction) (Fig. 1b and c). In addition, we also noticed that, during the awake state, frontal EEG showed broadband elevated high-frequency activities (Fig. 1c), which could be induced by muscle or eye movement.[39,40] Therefore, we excluded power and power-law analysis for awake EEG in further analysis.

We next investigated how general anaesthesia affects subcortical–cortical communication by evaluating the coherence between STN LFPs and frontal cortical EEG. Group-level imaginary coherence analysis (n=16; eight subjects) showed that, at LOR, there was a significant increase in STN–frontal cortex coherence, but only in the alpha range (8–13 Hz) (119 [68]%; P=0.0049) (Fig. 1d).

Temporal dynamics of neural activity in STN measured by power-law distribution is differential in awake and LOR states

The power spectra of the STN LFPs, plotted in a log–log coordinate space (Fig. 2a), roughly followed a straight descending line, with local peaks corresponding to well-known neural oscillations rising above this line. Figure 2a also shows the fractal components of the power spectra (after removing the oscillatory components) for an example LFP signal from STN at awake and LOR states. However, as broadband spectral peaks could not be removed completely, the remaining fractal components of the power spectrum still had a 'hump' in some frequency ranges, although reducing oscillatory activity. Therefore, we focused on the linear fitting of the fractal component of the power spectrum across a frequency range (2–80 Hz), excluding 8–40 Hz range, which covers most oscillatory activity (e.g. STN beta oscillation at awake and alpha oscillation at LOR). Group-level power-law exponents across all subjects (n=24; 12 subjects) estimated from the slope of the linear fitting for each tested STN showed that the averaged exponent value in the STN significantly increased from 1.12 (0.27) (range: 0.65–1.93) in awake state to 1.83 (0.29) (range: 1.26–2.22) in LOR state (P<0.0001) (Fig. 2b), indicating steeper reduction of power with increasing frequency in LOR.

Changes of neural activity in the STN induced by tracheal intubation in anaesthesia

Tracheal intubation is an arousal intervention in anaesthesia. Figure 3a shows representative spectrograms in the STN LFP and frontal EEG activity around tracheal intubation procedure under anaesthesia showing apparent increased beta activity in the STN at intubation. Group-level spectral analysis (n=20; 10 subjects) revealed a significant increase in beta and broadband high-gamma power in the STN (low beta: 21 [41]%, P=0.0257; high beta: 98 [123]%, P=0.0064; and high gamma: 10 [16]%, P=0.033; FDR correction). In comparison, we did not observe any significant changes over the frontal cortex comparing intubation against the status of loss of consciousness (Fig. 3b and c). The imaginary coherence between STN and frontal cortex showed slight but non-significant decrease in alpha band in intubation compared with LOR state (Fig. 3d).

Subsequently, the group-level time-variant powers in high-beta band in both STN and frontal cortex were computed by taking the mean across all subjects with the data aligned to the time points of LOR and tracheal intubation, respectively (Fig. 4). The group statistical analysis revealed that, compared with LOR state, the high-beta power dynamically increased in tracheal intubation in the STN, which was not observed in the cortex.

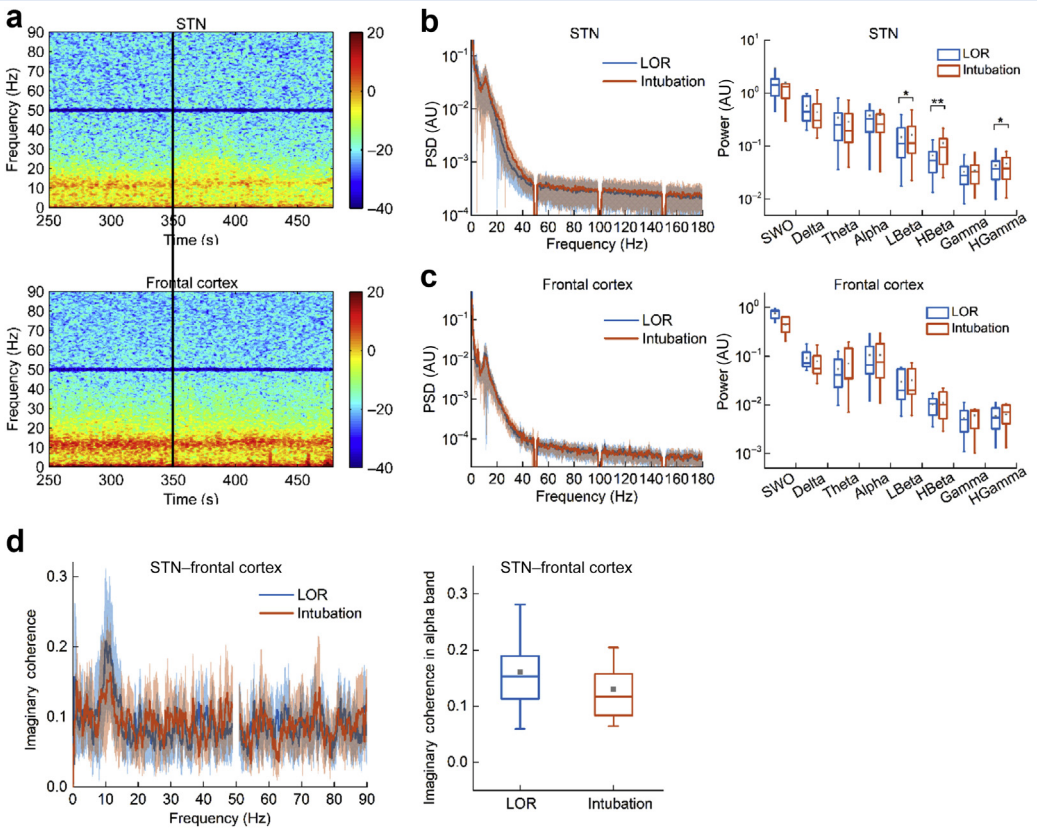

Figure 3. Intubation was associated with increased activity in the beta-frequency and broadband high-gamma band in the subthalamic nucleus (STN), but not over the frontal cortex. (a) Representative time–frequency spectrograms of STN local field potentials (LFPs) and frontal cortical EEG around intubation in anaesthesia. The vertical black line marks the time of starting intubation. (b) Group spectra and box plot showing power in different frequency bands of STN LFPs across subjects in loss of responsiveness (LOR) state. (c) Group spectra and box plot showing power in different frequency bands of STN LFPs across subjects in intubation state. (d) Group imaginary coherence between STN and frontal cortex across subjects in awake and LOR states. *P<0.05; **P<0.01. HBeta, high beta; HGamma, high gamma; LBeta, low beta; PSD, power spectral density; SWO, slow-wave oscillation.

Changes in power-law exponent in STN LFPs and frontal EEG induced by tracheal intubation

Compared with LOR state, the averaged power-law exponent (n=20; 10 subjects) significantly decreased from 1.83 (0.30) (range: 1.26–2.21) to 1.66 (0.30) (range: 1.09–1.97) at intubation state in the STN (P=0.0012; FDR correction) (Fig. 5a). However, the power-law exponent is still higher than that during awake (P<0.0001; FDR correction) (Fig. 5a), suggesting scaled changes in the power-law exponent of STN LFPs associated with different levels of consciousness and arousal during anaesthesia. However, the effect of tracheal intubation on the power-law exponent in frontal cortical EEG was non-significant (Fig. 5b). There were also much larger cross-subject variations in frontal cortex power-law exponent during awake. This was influenced by the remaining myogenic contamination in the awake EEG. Elevated power in high-frequency activities attributable to the myogenic contamination during awake led to negative values for the power-law exponent in some subjects. Moreover, time-resolved power-law exponent estimation showed that the power-law exponent reduced rapidly after tracheal intubation in anaesthesia, but remained higher than during awake (Supplementary Fig. S1a). The power at high-gamma frequency band varied in a coherent way that followed the power-law relationship (Supplementary Fig. S1b–d).

Discussion

In the present study, we used the unique opportunity afforded by synchronous electrophysiological recordings directly from human STN and frontal cortex to characterise changes in both oscillatory and arrhythmic activities in basal ganglia and cortical dynamics associated with consciousness in general anaesthesia. We showed that (i) unconsciousness state induced by propofol–sufentanil induced changes in multiple frequency bands in human STN LFP. These changes include increased oscillations in low frequencies, including SWO, delta, theta, and alpha bands, and reduced oscillation in beta-frequency band and reduced broadband high-frequency activity. There is also increased coherence between STN and frontal cortex, but only in the alpha band. (ii) The LFP power-law exponent in the STN between 2 and 80 Hz

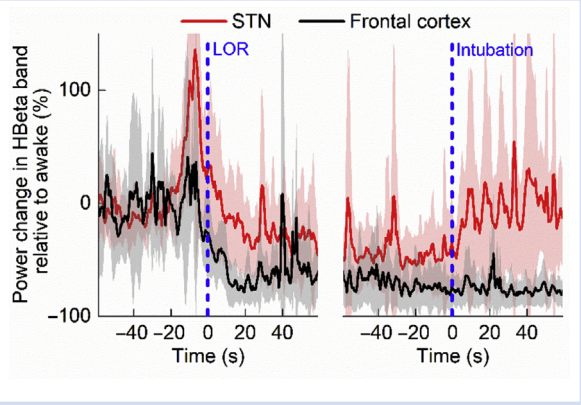

Figure 4. Group-level time-variant power in high-beta band of the electrophysiological signals recorded from the subthalamic nucleus (STN) and frontal cortex. The vertical dashed lines indicate the time of loss of responsiveness (LOR) and the time of tracheal intubation. HBeta, high beta.

significantly increased at LOR compared with awake state and temporally decreased after tracheal intubation, but it was still higher than the awake state. The dynamic changes in the power-law exponent correlated with fluctuation of broadband high-frequency activity. Our finding coincides with previous computational modelling and animal studies showing increased frontal corticothalamic alpha coherence associated with loss of consciousness.[15,41] Our results are also consistent with the previous study that showed reduced beta-band activity in STN during general anaesthesia.[25] Furthermore, our results highlighted specific changes in STN, including increase in beta and high-gamma power during tracheal intubation in anaesthesia, which were not observed in the cortical EEG.

Our study is novel in three ways. First, we revealed consistent variation of power-law distribution in the 2–80 Hz range in the PSD of STN LFPs in general anaesthesia. Most previous studies on the EEG, ECoG, and MEG recordings have focused on the narrowband oscillatory activities, treating the scale-free activities following the power law as recording noise. The power-law scaling of the PSD could be explained by different mechanisms according to different frequency ranges.[28,31] Recent evidence from computational modelling and *in vivo* recordings suggested that the power-law exponent in low-frequency bands reflects the balance between excitation and inhibition.[35] The balance between excitation and inhibition plays a crucial role in the brain functioning of neuronal networks,[42] and the power-law exponent in the cortical LFPs has been shown to be modulated in anaesthesia.[35,36,43] This is the first study, to our knowledge, which suggests that the power-law exponent in STN LFPs is consistently modulated by anaesthetic-induced unconsciousness in humans. This is also consistent with the hypothesis that the power-law exponent reflects excitation/inhibition balance. Propofol may have decreased the excitation/inhibition ratio in the STN in anaesthesia, which is reflected in the steeper power-law slope in the STN LFPs.

Second, we identified reduced broadband high-gamma activity in the STN in anaesthesia. Broadband high-frequency activity without a narrow power peak in the spectrum is considered a reflection of arrhythmic activity,[31] and has been suggested to potentially reflect the local population firing activity[44] or with neuronal spiking rate.[45,46] Thus, the attenuation of high-gamma power by propofol–sufentanil anaesthesia that we observed in the STN in this study likely reflects reduced neuronal firing rates in anaesthesia, which has been reported in recent studies using microelectrode recordings in the STN.[47,48]

In addition, we show that the dynamic temporal fluctuations in the power-law exponent in the lower-frequency band correlated with the changes in broadband high-frequency power, again supporting the hypothesis that anaesthesia can lead to changes in the excitation/inhibition balance in STN, which may in turn reduce nucleus output in the form of multi-unit activity. On the other hand, there was no correlation between high-frequency power and power of low-frequency activities (alpha band) during anaesthesia (not shown), which was suggested to be a neural correlate of synchronised afferent input to the nucleus.[45,49]

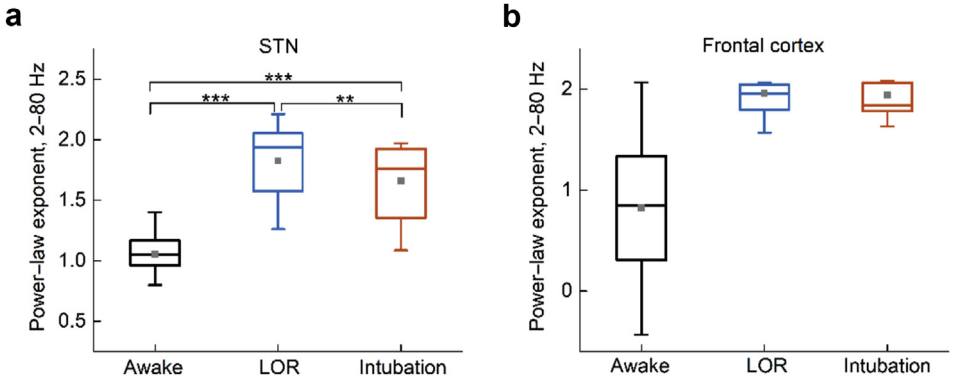

Figure 5. Power-law difference in subthalamic nucleus (STN) local field potentials (LFPs) and frontal EEG between different brain states. (a) Box plot showing power-law exponent in STN LFPs across subjects in awake, loss of responsiveness (LOR), and intubation states. (b) Box plot showing power-law exponent in frontal EEG across subjects in awake, LOR, and intubation states. **P<0.01; ***P<0.001.

Third, but not the least, we also investigated the changes of neural signatures in STN at intubation state during general anaesthesia. This is valuable, as clinically relevant noxious stimuli, such as tracheal intubation or skin incision, may induce intraoperative awareness.[50–52] Gaskell and colleagues[53] showed that volitional responses to verbal command could occur immediately after intubation in patients exhibiting an alpha–delta dominant (delta power >20 dB; alpha power >10 dB) EEG pattern, suggesting that frontal EEG parameters, such as alpha–delta power and bispectral index, do not readily discriminate volitional responsiveness and unresponsiveness during anaesthesia, as shown in several prospective RCTs.[54–57] Our findings from STN LFPs demonstrated that there were neural responses in the subcortical areas to tracheal intubation in anaesthesia, potentially advancing our understanding of intraoperative awareness in the future. The increase of beta-band activity in the STN during tracheal intubation, which was not observed in the frontal cortex, is consistent with the hypothesis that subcortical nuclei may serve the starter motors[13] for regaining responsiveness from propofol-induced sedation. Tracheal intubation increased activities in the STN, but may not be enough to trigger the phase-transition process for activating the cortical activity.

There are some limitations in this study. First, our experiments were conducted within clinical settings, in which anaesthetic management was administered according to the anaesthetist's discretion, rather than in a controlled, titrated manner. This prevented us from correlating the neural signatures with precise consciousness level. We mitigated these defects by examining the approximately steady states before and after induction of anaesthesia. Moreover, we used intubation state as an arousing intervention to investigate whether there was a reversal of the patterns, partially supporting the findings of biomarkers for consciousness, and the dynamic changes over time of these neural signatures were achieved by combining these measures and a time-windowing approach. Future studies would benefit from target-controlled infusion approach during induction of anaesthesia to have a detailed investigation of concentration-dependent effects featuring hierarchic states of consciousness. The other limitation of this study is a lack of isolated forearm technique (IFT) testing, which is a practical means of assessing responsiveness to command after intubation during anaesthesia in real time when neuromuscular blocking agents are used.[50,51,53] With this technique, it would have been possible to know with certainty whether or not subjects had (briefly) regained responsiveness after tracheal intubation. This could be evaluated using IFT in further studies. In addition, the electrophysiological recordings were from PD patients in this study, raising a consideration of whether the reported changes in the STN were related to PD symptoms. However, the patients were on medication for controlling PD symptoms during recording, partly mitigating the effect of the disease. In addition, the effects of propofol on STN activity were highly consistent with those observed in cortical areas. This suggests that the reported characteristics here are likely to partly generalise to the healthy brain. It should also be acknowledged that the power-law exponent quantified in this study is not independent from the power of different sub-frequency bands, including alpha, beta, and mid-gamma bands. However, the power-law exponent takes into account the relationship between the powers of different frequency bands, and can provide an estimate of the high-gamma activity. In addition, the frontal EEG recordings were contaminated by myogenic activity, preventing from investigating the characteristics related to high frequencies in the EEG. In further studies, multi-channel EEG recordings and blind source separation algorithm can be used to remove the artefacts.[58,59]

In conclusion, we characterised STN neural activity from two profiles, including oscillatory features and non-oscillatory (scale-free) features during anaesthesia. These findings provide important electrophysiological evidence in humans of the neural mechanisms regarding basal ganglia for propofol/sufentanil-induced unresponsiveness.

Authors' contributions

Study design: YH, KH, HT
Data collection: YH, KH, ALG, XM, MJG, JJF, YP, SM, PH, SZ, DL, TZA, BS
Data analysis: YH, HT
Data interpretation: all authors
Drafting of manuscript: YH, HT
Revising of manuscript: all authors

Declarations of interest

The authors declare that they have no conflicts of interest.

Funding

Shanghai Pujiang Program (19PJ1407500) to KH; Medical and Engineering Cross Research Fund from Shanghai Jiao Tong University (YG2019QNA31) to KH; Shanghai Municipal Health Commission Clinical Study Special Fund (20194Y0067) to KH; Ruijin Hospital Guangci Excellence Youth Training Program (GCQN-2019-B10) to KH; Ruijin Youth Natural Science Foundation of China Cultivation Fund (2019QNPY01031) to KH; National Institute for Health Research Oxford Biomedical Research Centre to YH; Shanghai Municipal Science and Technology Major Project (2018SHZDZX01) and ZJLab to SW; National Natural Science Foundation of China (81471482) to BS; Shanghai Jiao Tong University School of Medicine–Institute of Neuroscience Research Center for Brain Disorders to BS; Academy of Medical Sciences, Starter Grant for Clinical lecturers to MJG; National Institute for Health Research Academy (Ref. CL-2013-13-001) to MJG.

Acknowledgements

The authors acknowledge Simon Yarrow for conducting anaesthesia on some of the patients, and Peter Brown for constructive and critical comments. The scheme is generously supported by the Wellcome Trust, Medical Research Council, British Heart Foundation, Versus Arthritis, Diabetes UK, and British Thoracic Society (through the Helen and Andrew Douglas bequest). The views expressed are those of the authors and not necessarily those of the National Institute for Health Research, National Health Service, or the Department of Health and Social Care.

Appendix A. Supplementary data

Supplementary data to this article can be found online at https://doi.org/10.1016/j.bja.2020.03.014.

References

1. Purdon PL, Pierce ET, Mukamel EA, et al. Electroencephalogram signatures of loss and recovery of consciousness from propofol. *Proc Natl Acad Sci U S A* 2013; **110**: E1142–51
2. Ni Mhuircheartaigh R, Warnaby C, Rogers R, Jbabdi S, Tracey I. Slow-wave activity saturation and thalamocortical isolation during propofol anesthesia in humans. *Sci Transl Med* 2013; **5**. 208ra148
3. John E, Prichep L, Kox W, et al. Invariant reversible QEEG effects of anesthetics. *Conscious Cogn* 2001; **10**: 165–83
4. Akeju O, Pavone KJ, Westover MB, et al. A comparison of propofol- and dexmedetomidine-induced electroencephalogram dynamics using spectral and coherence analysis. *Anesthesiology* 2014; **121**: 978–89
5. Huotari AM, Koskinen M, Suominen K, et al. Evoked EEG patterns during burst suppression with propofol. *Br J Anaesth* 2004; **92**: 18–24
6. Bruhn J, Bouillon TW, Shafer SL. Onset of propofol-induced burst suppression may be correctly detected as deepening of anaesthesia by approximate entropy but not by bispectral index. *Br J Anaesth* 2001; **87**: 505–7
7. Fiset P, Paus T, Daloze T, et al. Brain mechanisms of propofol-induced loss of consciousness in humans: a positron emission tomographic study. *J Neurosci* 1999; **19**: 5506–13
8. White NS, Alkire MT. Impaired thalamocortical connectivity in humans during general-anesthetic-induced unconsciousness. *Neuroimage* 2003; **19**: 402–11
9. Brown EN, Purdon PL, Van Dort CJ. General anesthesia and altered states of arousal: a systems neuroscience analysis. *Annu Rev Neurosci* 2011; **34**: 601–28
10. Boveroux P, Vanhaudenhuyse A, Bruno MA, et al. Breakdown of within- and between-network resting state functional magnetic resonance imaging connectivity during propofol-induced loss of consciousness. *Anesthesiology* 2010; **113**: 1038–53
11. Lee U, Ku S, Noh G, Baek S, Choi B, Mashour GA. Disruption of frontal-parietal communication by ketamine, propofol, and sevoflurane. *Anesthesiology* 2013; **118**: 1264–75
12. Nir T, Or-Borichev A, Izraitel E, Hendler T, Lerner Y, Matot I. Transient subcortical functional connectivity upon emergence from propofol sedation in human male volunteers: evidence for active emergence. *Br J Anaesth* 2019; **123**: 298–308
13. Sleigh J, Warnaby CE. Finding the starter motor for the engine of consciousness. *Br J Anaesth* 2019; **123**: 259–61
14. Huang Y, Wu D, Bahuri NFA, et al. Spectral and phase-amplitude coupling signatures in human deep brain oscillations during propofol-induced anaesthesia. *Br J Anaesth* 2018; **121**: 303–13
15. Flores FJ, Hartnack KE, Fath AB, et al. Thalamocortical synchronization during induction and emergence from propofol-induced unconsciousness. *Proc Natl Acad Sci U S A* 2017; **114**: E6660–8
16. Verdonck O, Reed SJ, Hall J, Gotman J, Plourde G. The sensory thalamus and cerebral motor cortex are affected concurrently during induction of anesthesia with propofol: a case series with intracranial electroencephalogram recordings. *Can J Anaesth* 2014; **61**: 254–62
17. Zavala BA, Tan H, Little S, et al. Midline frontal cortex low-frequency activity drives subthalamic nucleus oscillations during conflict. *J Neurosci* 2014; **34**: 7322–33
18. Kelley R, Flouty O, Emmons EB, et al. A human prefrontal-subthalamic circuit for cognitive control. *Brain* 2018; **141**: 205–16
19. Aziz TZ, Davies L, Stein J, France S. The role of descending basal ganglia connections to the brain stem in Parkinsonian akinesia. *Brit J Neurosurg* 1998; **12**: 245–9
20. Takakusaki K, Saitoh K, Harada H, Kashiwayanagi M. Role of basal ganglia-brainstem pathways in the control of motor behaviors. *Neurosci Res* 2004; **50**: 137–51
21. Mhuircheartaigh RN, Rosenorn-Lanng D, Wise R, Jbabdi S, Rogers R, Tracey I. Cortical and subcortical connectivity changes during decreasing levels of consciousness in humans: a functional magnetic resonance imaging study using propofol. *J Neurosci* 2010; **30**: 9095–102
22. Qiu MH, Vetrivelan R, Fuller PM, Lu J. Basal ganglia control of sleep-wake behavior and cortical activation. *Eur J Neurosci* 2010; **31**: 499–507
23. Crone JS, Lutkenhoff ES, Bio BJ, Laureys S, Monti MM. Testing proposed neuronal models of effective connectivity within the cortico-basal ganglia-thalamo-cortical loop during loss of consciousness. *Cereb Cortex* 2017; **27**: 2727–38
24. Weng L, Xie Q, Zhao L, et al. Abnormal structural connectivity between the basal ganglia, thalamus, and frontal cortex in patients with disorders of consciousness. *Cortex* 2017; **90**: 71–87
25. Martinez-Simon A, Alegre M, Honorato-Cia C, et al. Effect of dexmedetomidine and propofol on basal ganglia activity in Parkinson disease: a controlled clinical trial. *Anesthesiology* 2017; **126**: 1033–42
26. He BJ, Zempel JM, Snyder AZ, Raichle ME. The temporal structures and functional significance of scale-free brain activity. *Neuron* 2010; **66**: 353–69
27. Buzsaki G, Anastassiou CA, Koch C. The origin of extracellular fields and currents—EEG, ECoG, LFP and spikes. *Nat Rev Neurosci* 2012; **13**: 407–20
28. He BJ. Scale-free brain activity: past, present, and future. *Trends Cogn Sci* 2014; **18**: 480–7
29. Wen H, Liu Z. Broadband electrophysiological dynamics contribute to global resting-state fMRI signal. *J Neurosci* 2016; **36**: 6030–40
30. Freeman WJ, Zhai J. Simulated power spectral density (PSD) of background electrocorticogram (ECoG). *Cogn Neurodyn* 2009; **3**: 97–103
31. Miller KJ, Sorensen LB, Ojemann JG, den Nijs M. Power-law scaling in the brain surface electric potential. *PLoS Comput Biol* 2009; **5**, e1000609
32. Miskovic V, MacDonald KJ, Rhodes LJ, Cote KA. Changes in EEG multiscale entropy and power-law frequency scaling during the human sleep cycle. *Hum Brain Mapp* 2019; **40**: 538–51
33. Maxim V, Sendur L, Fadili J, et al. Fractional Gaussian noise, functional MRI and Alzheimer's disease. *Neuroimage* 2005; **25**: 141–58
34. Tolkunov D, Rubin D, Mujica-Parodi L. Power spectrum scale invariance quantifies limbic dysregulation in trait anxious adults using fMRI: adapting methods optimized for characterizing autonomic dysregulation to neural dynamic time series. *Neuroimage* 2010; **50**: 72–80
35. Gao R, Peterson EJ, Voytek B. Inferring synaptic excitation/inhibition balance from field potentials. *Neuroimage* 2017; **158**: 70–8
36. Colombo MA, Napolitani M, Boly M, et al. The spectral exponent of the resting EEG indexes the presence of

consciousness during unresponsiveness induced by propofol, xenon, and ketamine. *Neuroimage* 2019; **189**: 631–44
37. Bokil H, Andrews P, Kulkarni JE, Mehta S, Mitra PP. Chronux: a platform for analyzing neural signals. *J Neurosci Methods* 2010; **192**: 146–51
38. Wen H, Liu Z. Separating fractal and oscillatory components in the power spectrum of neurophysiological signal. *Brain Topogr* 2016; **29**: 13–26
39. Whitham EM, Pope KJ, Fitzgibbon SP, et al. Scalp electrical recording during paralysis: quantitative evidence that EEG frequencies above 20 Hz are contaminated by EMG. *Clin Neurophysiol* 2007; **118**: 1877–88
40. Yuval-Greenberg S, Tomer O, Keren AS, Nelken I, Deouell LY. Transient induced gamma-band response in EEG as a manifestation of miniature saccades. *Neuron* 2008; **58**: 429–41
41. Ching S, Cimenser A, Purdon PL, Brown EN, Kopell NJ. Thalamocortical model for a propofol-induced alpha-rhythm associated with loss of consciousness. *Proc Natl Acad Sci U S A* 2010; **107**: 22665–70
42. Hensch TK. Critical period plasticity in local cortical circuits. *Nat Rev Neurosci* 2005; **6**: 877–88
43. Muthukumaraswamy SD, Liley DT. 1/f Electrophysiological spectra in resting and drug-induced states can be explained by the dynamics of multiple oscillatory relaxation processes. *Neuroimage* 2018; **179**: 582–95
44. Buzsaki G, Silva FL. High frequency oscillations in the intact brain. *Prog Neurobiol* 2012; **98**: 241–9
45. Ray S, Crone NE, Niebur E, Franaszczuk PJ, Hsiao SS. Neural correlates of high-gamma oscillations (60–200 Hz) in macaque local field potentials and their potential implications in electrocorticography. *J Neurosci* 2008; **28**: 11526–36
46. Ray S, Maunsell JH. Different origins of gamma rhythm and high-gamma activity in macaque visual cortex. *PLoS Biol* 2011; **9**, e1000610
47. Raz A, Eimerl D, Zaidel A, Bergman H, Israel Z. Propofol decreases neuronal population spiking activity in the subthalamic nucleus of Parkinsonian patients. *Anesth Analg* 2010; **111**: 1285–9
48. Kwon WK, Kim JH, Lee JH, et al. Microelectrode recording (MER) findings during sleep–awake anesthesia using dexmedetomidine in deep brain stimulation surgery for Parkinson's disease. *Clin Neurol Neurosurg* 2016; **143**: 27–33
49. Kreiman G, Hung CP, Kraskov A, Quiroga RQ, Poggio T, DiCarlo JJ. Object selectivity of local field potentials and spikes in the macaque inferior temporal cortex. *Neuron* 2006; **49**: 433–45
50. Sanders RD, Tononi G, Laureys S, Sleigh JW. Unresponsiveness not equal unconsciousness. *Anesthesiology* 2012; **116**: 946–59
51. Sanders RD, Gaskell A, Raz A, et al. Incidence of connected consciousness after tracheal intubation: a prospective, international, multicenter cohort study of the isolated forearm technique. *Anesthesiology* 2017; **126**: 214–22
52. Zbinden AM, Maggiorini M, Petersen-Felix S, Lauber R, Thomson DA, Minder CE. Anesthetic depth defined using multiple noxious stimuli during isoflurane/oxygen anesthesia. I. Motor reactions. *Anesthesiology* 1994; **80**: 253–60
53. Gaskell AL, Hight DF, Winders J, et al. Frontal alpha-delta EEG does not preclude volitional response during anaesthesia: prospective cohort study of the isolated forearm technique. *Br J Anaesth* 2017; **119**: 664–73
54. Myles PS, Leslie K, McNeil J, Forbes A, Chan MT. Bispectral index monitoring to prevent awareness during anaesthesia: the B-Aware randomised controlled trial. *Lancet* 2004; **363**: 1757–63
55. Avidan MS, Zhang L, Burnside BA, et al. Anesthesia awareness and the bispectral index. *N Engl J Med* 2008; **358**: 1097–108
56. Avidan MS, Jacobsohn E, Glick D, et al. Prevention of intraoperative awareness in a high-risk surgical population. *N Engl J Med* 2011; **365**: 591–600
57. Mashour GA, Shanks A, Tremper KK, et al. Prevention of intraoperative awareness with explicit recall in an unselected surgical population: a randomized comparative effectiveness trial. *Anesthesiology* 2012; **117**: 717–25
58. Fitzgibbon SP, DeLosAngeles D, Lewis TW, et al. Automatic determination of EMG-contaminated components and validation of independent component analysis using EEG during pharmacologic paralysis. *Clin Neurophysiol* 2016; **127**: 1781–93
59. Yilmaz G, Budan AS, Ungan P, Topkara B, Turker KS. Facial muscle activity contaminates EEG signal at rest: evidence from frontalis and temporalis motor units. *J Neural Eng* 2019; **16**, 066029

Handling editor: Tony Absalom